Contribution of multispectral remote sensing to mining exploration in the Rehamna Massif, Moroccan Meseta

Mohamed El-Mimouni[1,*], *Abdellatif* Aarab[1], *Abdellah* Lakhloufi[1], *Abderrazak* Hamzaoui[2], *Ahmed* Akhssas[3], *Kawtar* Benyas[1]

[1] Laboratoire Analyse et Modélisation de l'Eau et Ressources Naturelles (LAMERN) – EMI, centre de recherche CERNE2D, Université Mohamed V- ENS Rabat, Maroc
[2] Office Nationale des Hydrocarbures et des Mines (ONHYM), Rabat, Maroc
[3]Laboratoire de Géophysique Appliquée, de Géotechnique, de Géologie de l'Ingénieur et de l'Environnement (L3GIE), Ecole Mohammadia d'Ingénieurs, Université Mohamed V, Rabat, Maroc

Abstract. The Western Moroccan Meseta contains mining sites in operation for several decades and others in development. The Rehamna Massif belonging to this, is the subject of this study. The present study reveals new results on the mineralization in this massif. It is based on the synergy of field investigation data and ASTER image analysis (L1T) covering this massif. Through spectral processing, namely the calculation of the band ratios, ACP and MNF, applied to the nine VNIR and SWIR bands of this image, it was possible to reveal the distribution of hydrothermal alteration minerals in the study area. The conjuncture of these data allowed us to select geological targets likely to be of potential mining interest in the massif**.**

Key words : Rehamna Massif, mining exploration, ASTER image, field investigation.

1. Introduction

Except the phosphate deposits on its borders (Cenozoic cover), the Hercynian Rehamna Massif does not contain lot of current mining activity, unlike the other massifs of the Western Meseta, although they have a common geological history. Admittedly, the outcrops in this massif do not lend themselves well to direct observation; fact that prompted us to use other methods and techniques of investigation to get geo-mining information in this site.

Our study is based on the zones of hydrothermal alteration mapping by the identification of the minerals resulting from this phenomenon, namely kaolinite, chlorite, allunite and epidote using the opportunities offered by the multispectral satellite imagery. Several studies have shown the importance of mapping hydrothermal alteration minerals in mining exploration and identification of mining deposits [1- 3].

The images generated by the multi and hyper-spectral sensors have shown great utility in geological and mineral mapping, and therefore offer a decision support tool upstream of any mining exploration project. The use of these images in the detection of mining sites has become fruitful after the launch of the ETM + (Enhanced Themaic Mapper plus) and ASTER (Advanced Spectral Thermal Emission and Reflection Radiometer) satellites in 1999 [1, 4, 5].

2. Geological setting

The Rehamna Massif is located in the center of the Western Moroccan Meseta, in the middle position between the Moroccan Central Massif to the north and the Jebilet domain to the south. It is a segment of the Hercynian belt, containing Paleozoic formations, intruded by late hercynian granitic bodies, and covered, in part, by discordant, Meso-Cenozoic and Quaternary formations [6 - 9].

* elmimouni2@gmail.com

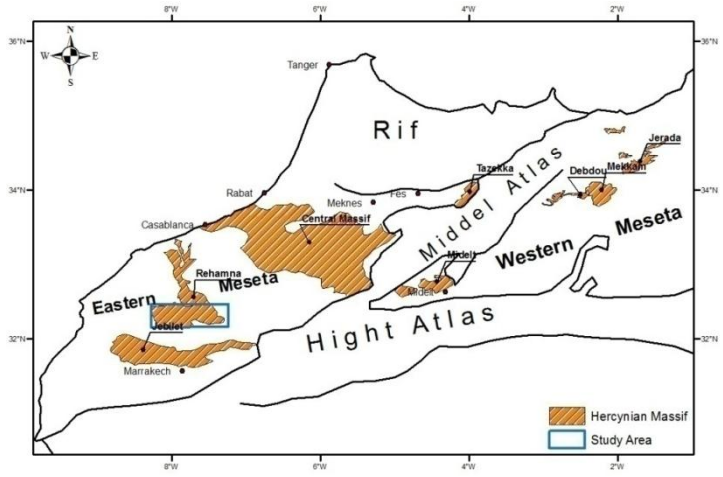

Fig.1. General map of the Moroccan mesetian domain (Northern Provinces of Morocco, extracted from the geological map 1000000^{e}).

In the Rehamna, the authors distinguish two parts: the North Rehamna or the Mechraa Ben Abbou basin and the Southern Rehamna or Rehamna s.str [6, 7]. The Rehamna s.str, object of this study, is subdivided into three structural zones: i) The Western Rehamna, part belonging to the coastal bloc, the least deformed zone of the Moroccan Meseta. This zone consists of Combro-Ordovician terrains limited to the east by the NNE-SSW median fault [10]. ii) The Central Rehamna, a narrow NE-SW band, between the Oulad Zednes shear zone in the east and the median fault in the west. This part of the Rehamna contains ortho-gneisses [8, 11, 12] dated from the Upper Precambrian [13] covered by Cambrian arkoses, limestones and cipolin, surmounted by the metaconglomerate of kef Elmounib [14] attributed to the lower Devonian, followed by Devonian terrains of Skhour containing phyllites and quartzites [12,15]. iii) Eastern Rehamna, zone limited to the west by the Oulad Zednes fault, and represented by two metamorphic units: lower unit of Lalla Tittaf and upper unit of Ouled Hassine. The first consists of micaschists, marbles and quartzites is attributed to probable Devonian [6, 12, 16], however, the age of Lalla Tittaf formation is controversial. It is constituted of micaschists with amphibolites, metagabbros, rare acid meta-tuffs and some levels of marbles [17] is attributed to the Lower Carboniferous (Viséen-Namurian) [6, 17]. However, zircon dating attributes this formation to Paleoproterozoic [12, 13].

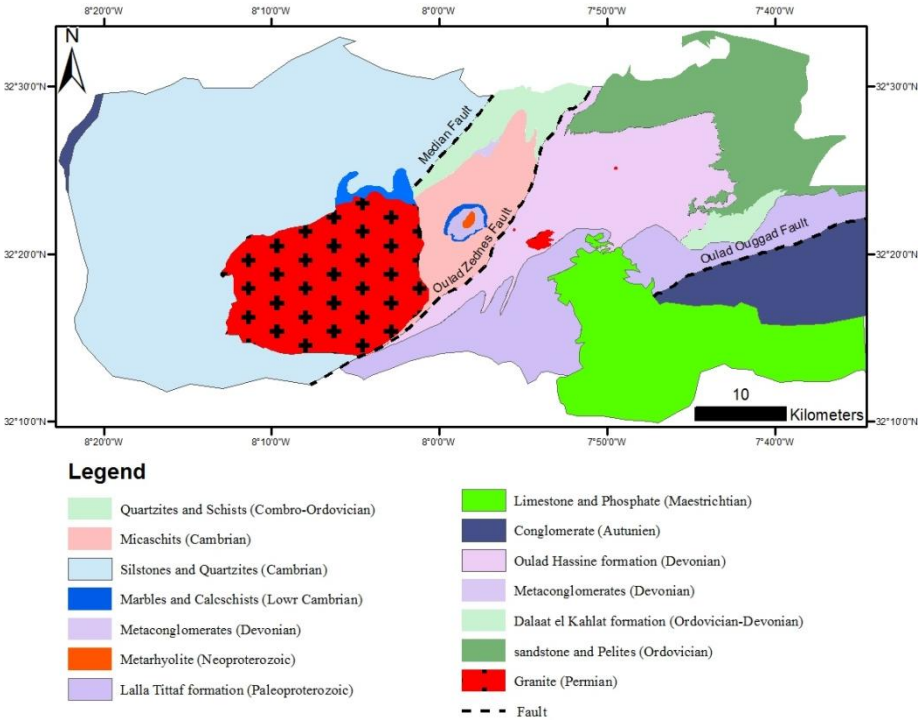

Fig.2. Simplified geological map of the Rehamna Massif (adapted from Gigout, 1951; Baudin et al.., 2003).

* elmimouni2@gmail.com

3. Ore deposit in the Rehamna massif

The Rehamna Massif, zone of the province with perbatholitic mineralization in the Hercynian domain, has been involved in mineral exploration for several decades [18, 19]. It can be traced back to the Roman era [12]. This works led to mining Sn, W, Be, Cu and Mo [20]. Many abandoned mines since the 1970s are known, mainly belonging to the Devonian unit of the Oulad Hassine of the East Rehamna: - the Oulad Hassine Plomb-Zinc mine; - the Raichet Wolfram mine ; and - Ouled Salah Barytine and Plomb mine. We also know several mining indices, namely Uranium, Beryl, Copper and Barytine. These Hercynian late-Hercynian mineralizations, generally vein-type, of pneumatolytic and hydrothermal origin, are essentially related to magmatic intrusions [21]. [22] Used, for the first time in the Rehamna, the remote sensing technique by means of Landsat MSS image for the prospection of tungsten mineralized leucogranitic apexes, by using of phenomenon of "transparency" of the cover metamorphic.

Until now, all data indicate that the mineralization discovered in the Rehamna Massif is essentially related to granitic intrusions, and is concentrated east of the Oulad Zednes Accident.

4. Data and method

In order to conduct the geological investigations, we relied on the ASTER satellite image data. The reputation of these data in the mining targeting and exploration as well as the sensitivity of certain bands to alteration minerals justify our use of it. In the present study, the ASTER level L1T image (AST_L1T_00303012007112752_6821), (Path 202 - Row 38), acquired on March 01 2007, is used. This data orthorectified and projected in the WGM-1984 system, obtained on the site of the United States Geological Survey (USGS). It composed of three bands in the near-infrared visible (VNIR), six bands in the short-wave infrared (SWIR) and five bands in the thermal-infrared (TIR) (Table 1).

The analysis of the image included three spectral methods applied to the nine VNIR and SWIR bands: first, band-ratio calculations to identify hydrothermal alteration minerals from possible zones with mining potential, then principal component analysis (PCA) and a minimum noise fraction transformation (MNF) were applied on the same bands to highlight selected areas.

Table 1. Spectral passbands of ASTER image.

Sybsystem	Band no.	Spectral range (µm)	Spatial resolution (m)
VNIR	1	0.52 - 0.60	15
	2	0.63 – 0.69	
	3N	0.76 – 0.86	
SWIR	4	1.60 – 1.70	30
	5	2.145 – 2.185	
	6	2.185 – 2.225	
	7	2.235 – 2.285	
	8	2.295 – 2.365	
	9	2.360 – 2.430	
TIR	10	8.125 – 8.475	90
	11	8.475 – 8.825	
	12	8.925 – 9.275	
	13	10.25 – 10.95	
	14	10.95 – 11.65	

* elmimouni2@gmail.com

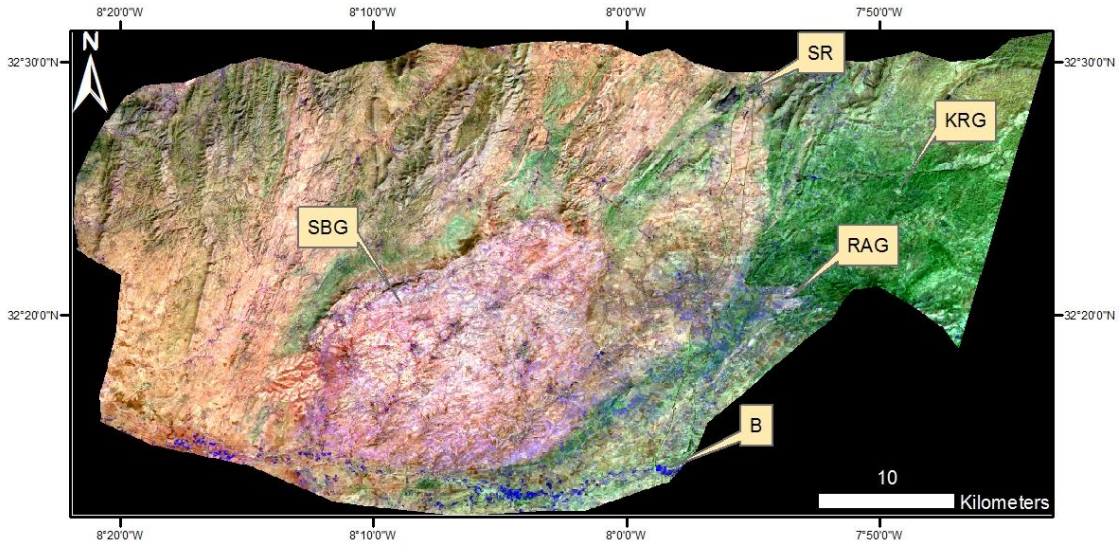

Fig. 3. False composite ASTER image (RGB 7-2-3) used in the study shown the Rehamna massif s.st (SBG : Sebt Brikiin granit, RAG: Ras Albioud granit, KRG: Koudiat Rmel granit, SR : Skhour Rehamna, B : Benguerir).

5. Data processing

5.1. Bands ratios

Band ratios are used in geology to discriminate types of rocks or minerals. The principle is to execute arithmetic operations on the digital number (DN) of each pixel of the bands considered in ratio. Several band ratios have been developed to highlight certain minerals or groups of minerals. Fig. 4 shows that the iron oxides (hematite, geothite) are detectable by bands 1 and 3, the Al-OH group of clay minerals by bands 5 and 6, band 7 detects Fe-OH (jarosite, muscovite) and band 8 detects Mg-OH (chlorite, epidote, carbonates) [23].

In our case study, we used the ratios of [24]; (Band 4 + Band 6) / Band 5 for the argillic zone (Allunite, kaolinite, Pyrophylite), (Band 7 + Band 9) / Band 8 for the prophylactic zone (Carbonate, Chlorite, Epidote) and (Band 5 / Band 3 + Band 1 / Band 2) for the oxidation zone (Fe2 +), as well as the ratio (Band 5 + Band 7) / Band 6 for the phyllic zone (Sericite, Muscovite, Illite, Smectite) [25]). The results of this methode are shown in Figure 5.

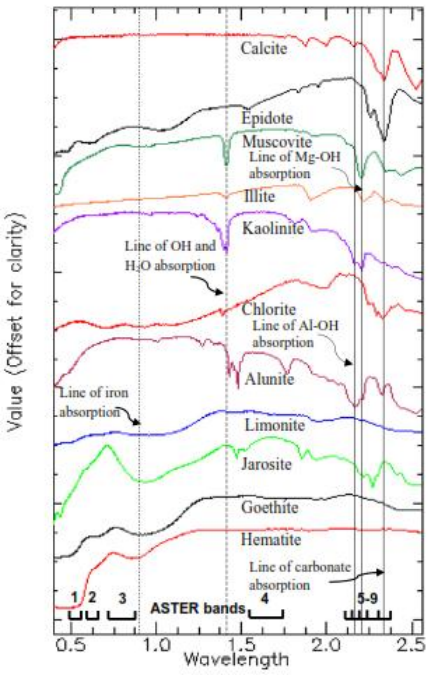

Fig.4. Laboratory spectra of minerals of hydrothermal alteration zones stacked from the USGS spectral library for minerals (in [23]).

* elmimouni2@gmail.com

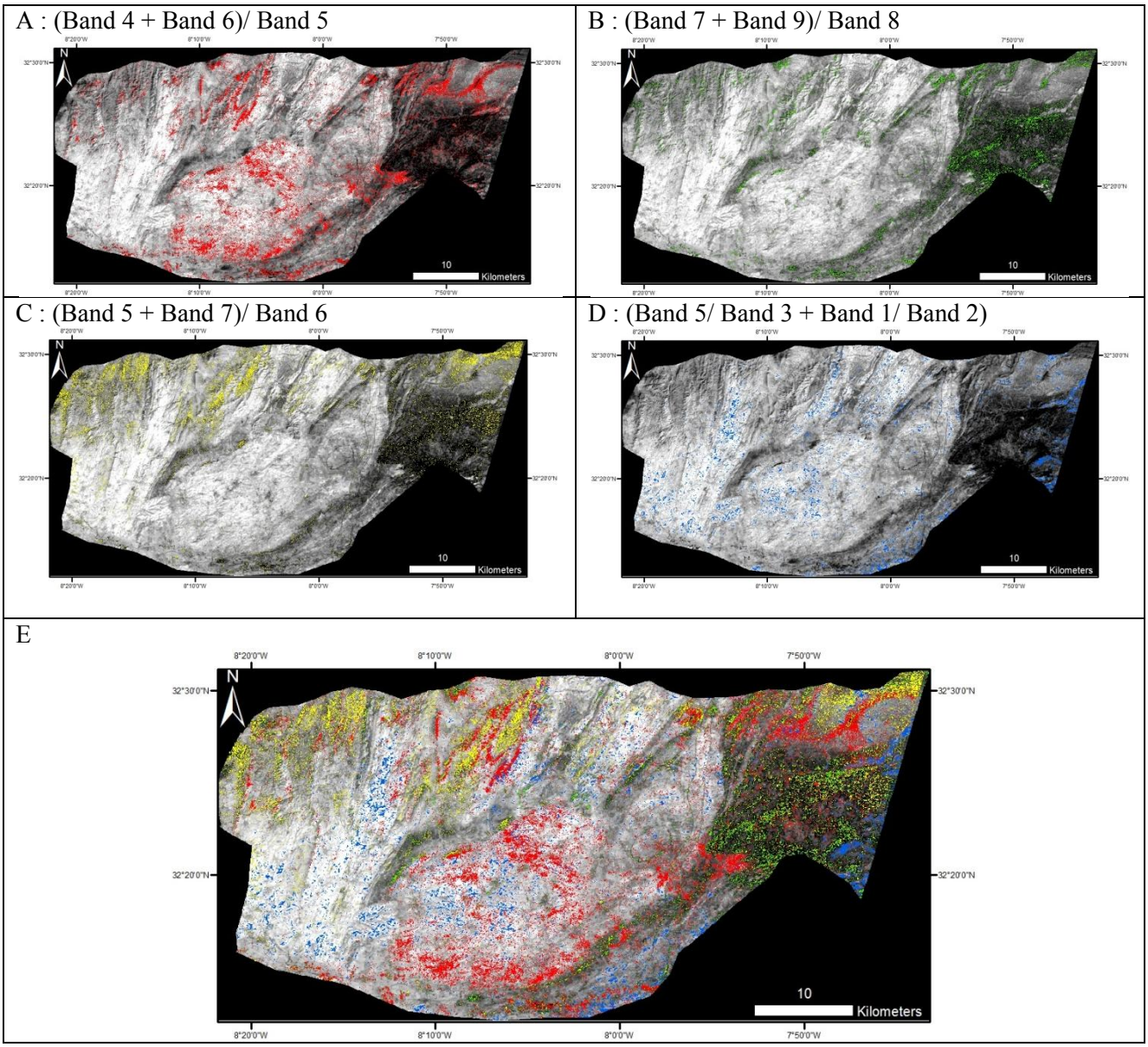

Fig.5. Maps of bands ratios studied (A to D), E resulting map.

We also tested the band ratios proposed by [26]: OHI, KLI, ALI and CLI index; with:

$$OHI = \left(\frac{Band7}{Band6}\right) * \left(\frac{\text{Band4}}{\text{Band6}}\right)$$

$$KLI = \left(\frac{Band4}{Band5}\right) * \left(\frac{\text{Band8}}{\text{Band6}}\right)$$

$$CLI = \left(\frac{Band6}{Band8}\right) * \left(\frac{\text{Band9}}{\text{Band8}}\right)$$

$$ALI = \left(\frac{Band7}{Band5}\right) * \left(\frac{\text{Band7}}{\text{Band8}}\right)$$

Where *OHI* is the mineral alteration index, *KLI* is the kaolinite index, *ALI* is the allunite index, and *CLI* is the index of calcite. Figure 6 shows the results of these ratios.

* elmimouni2@gmail.com

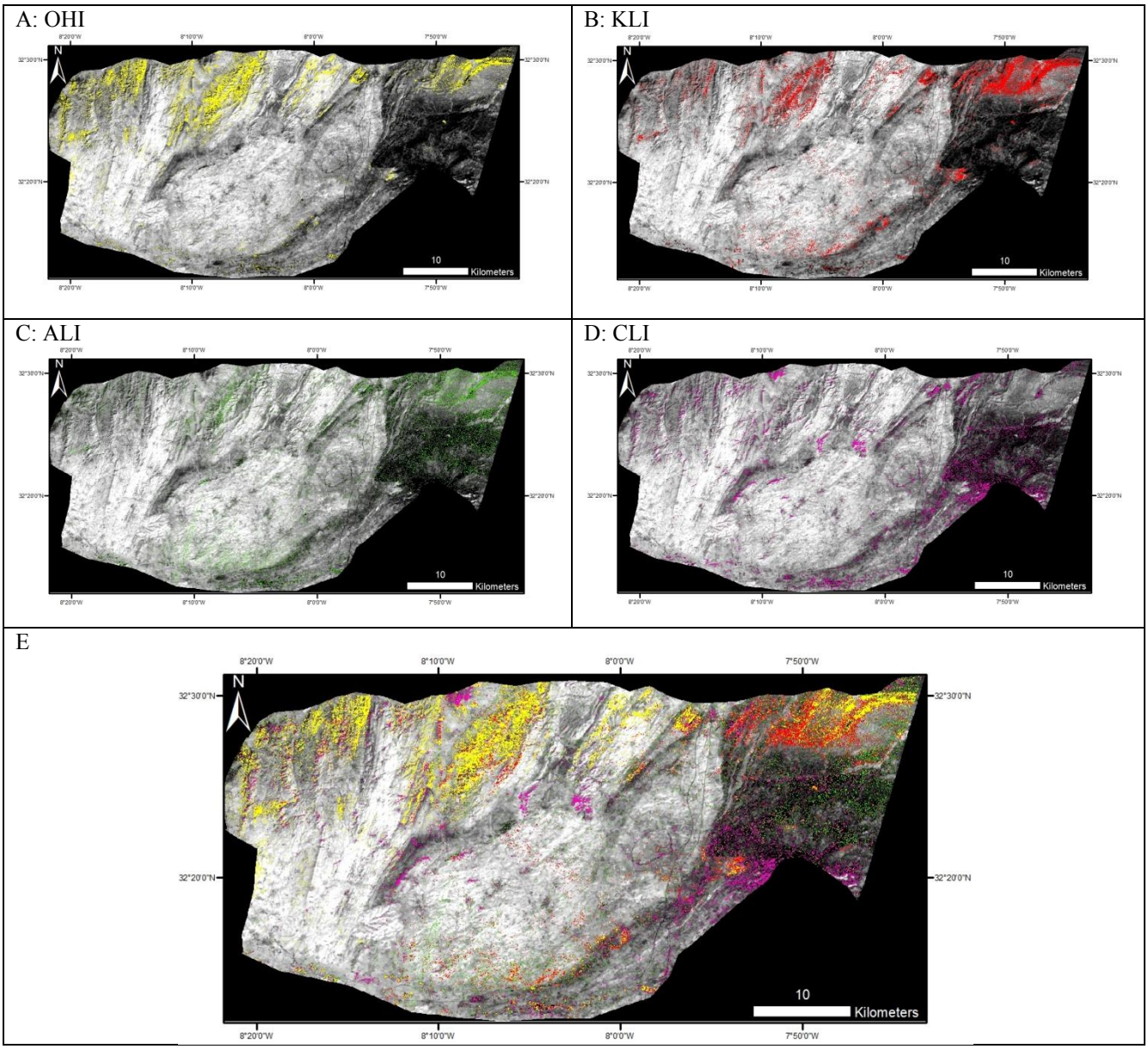

Fig. 6. Maps OHI, KLI, ALI, CLI bans ratio (A to D), E resulting map.

The compilation of the data obtained by the band-ratio method (Figure 5 and Figure 6) reveals a distribution of alteration minerals over the northern part of the study area. It's positioned between latitude 32 ° 20'N and 32 ° 30'N. The areas that we considered interesting are mentioned on the map Figure.7. The surface dimension of the polygons thus limited varies between 1 and 20 km^2 approximately. These polygons relating to the alteration minerals are structurally located in relation to the faulted zones and in borders of the granites.

* elmimouni2@gmail.com

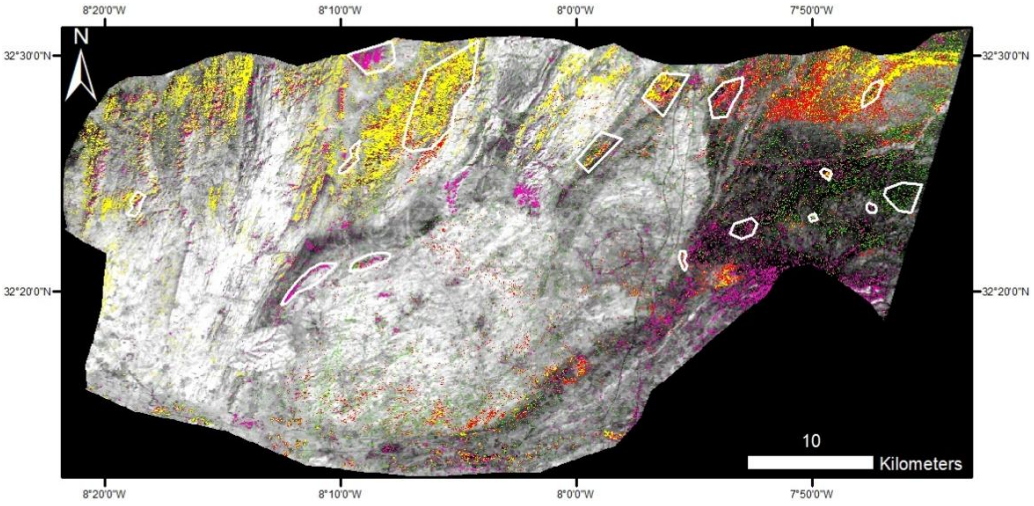

Fig.7. Map of selected areas using band ratio method.

5.2. PCA technique

Principal Component Analysis (PCA) is a multivariate statistical decomposition that consists in transforming correlated variables into new variables uncorrelated [27], with concentration of most of the spectral information in the first components. This technique is frequently used in alterations mapping field related to metallogenic provinces [28-30].

We applied this technique to our data using covariance matrix on all nine bands. Figure 8 shown the resulting components.

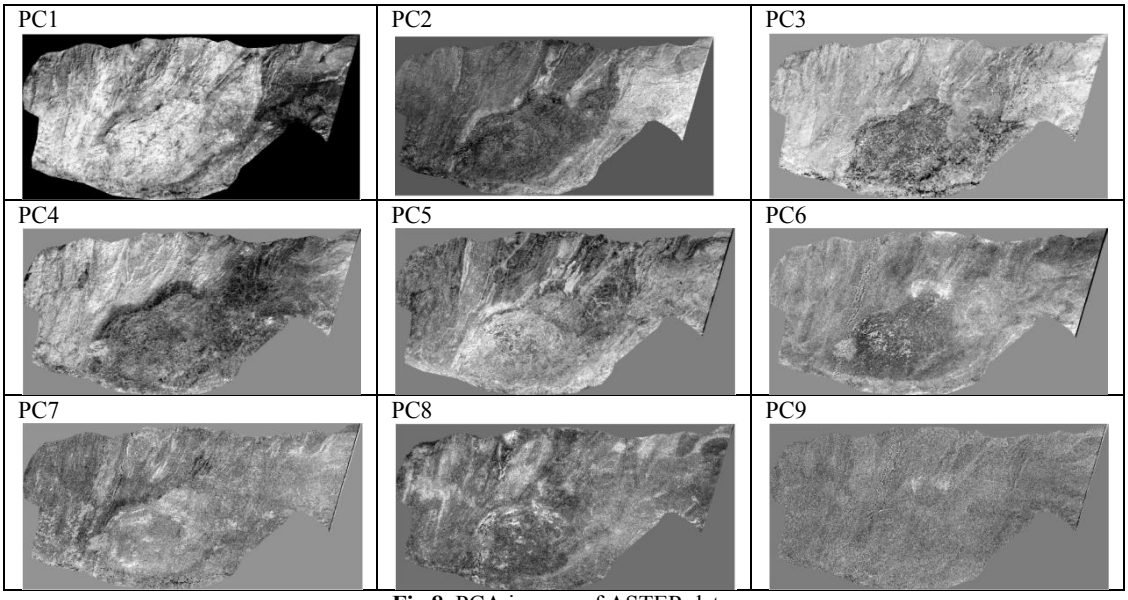

Fig.8. PCA images of ASTER data.

The image eigenvalues obtained from PCA are indicated in figure 9. The first three principal components (PC1, PC2, PC3) contain more than 90% of the spectral information, the last 3 components contain useless information.

* elmimouni2@gmail.com

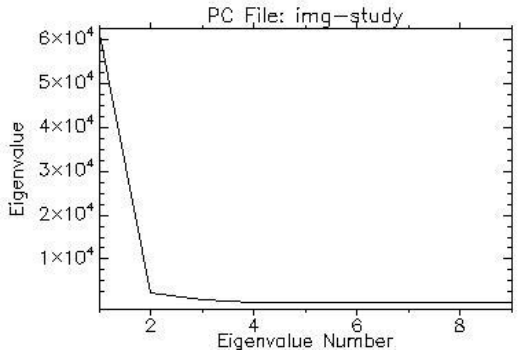

Fig.9. Eigenvalue of ASTER PCA image

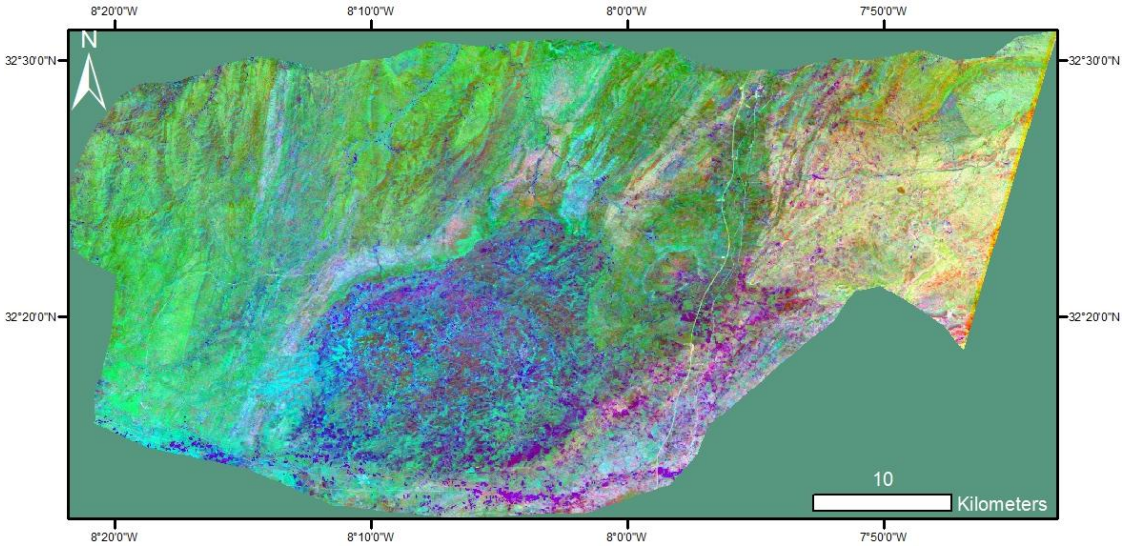

Fig.10. RGB colour combination of PCA 2-3-5 components

From PCA technique, we distinguish a good discrimination of the lithological facies of the study area. It allows to highlight the three structural units of the Rehamna Massif, the granitic bodies and the boundary between the Oulad Hassin and Lalla Tittaf units. Some areas of interest (figure 7) appear in dark purple

5.3. MNF technique

MNF (Minimum Noise Fraction) is a statistical transformation that is used to determine the inherent dimensionality of image data to isolate noise and reduce computational requirements for subsequent processing [31]. The first bands of this analysis contain useful spectral information, and the remaining bands contain noise [32].

The results of MNF technique applied to ASTER data of studied area are shown in figures 11-13.

* elmimouni2@gmail.com

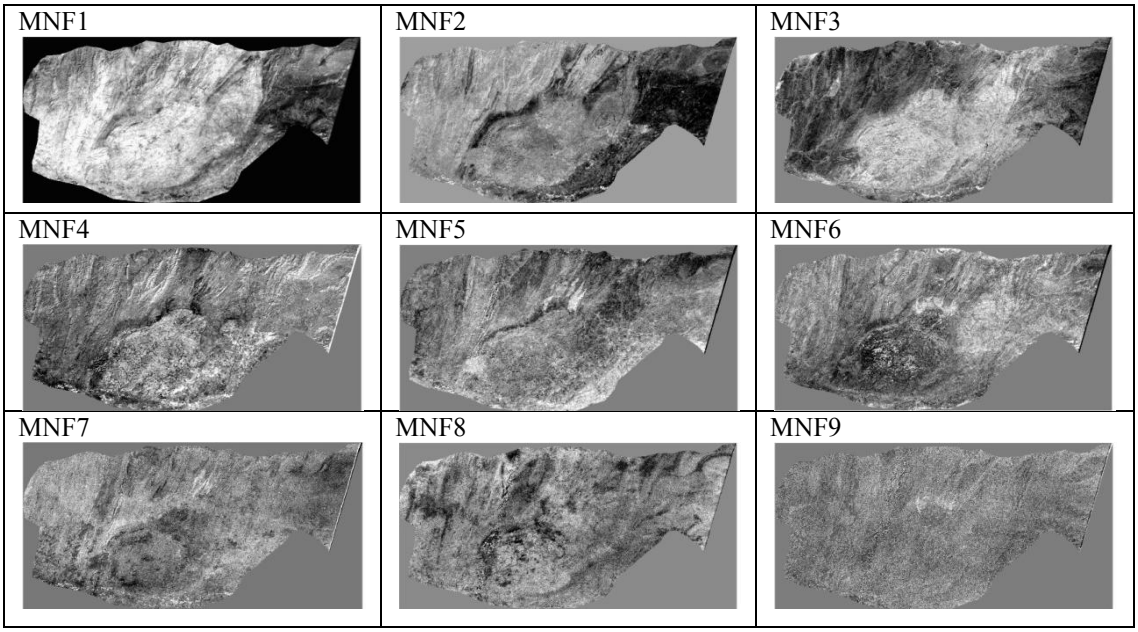

Fig.11. ASTER MNF images of area of study

The image eigenvalues obtained from MNF transformation are indicated in figure 12. The first images contain useful spectral information, and the last images are noised.

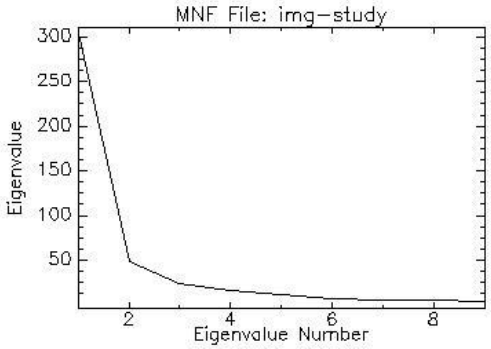

Fig.12. Eigenvalue of ASTER MNF image

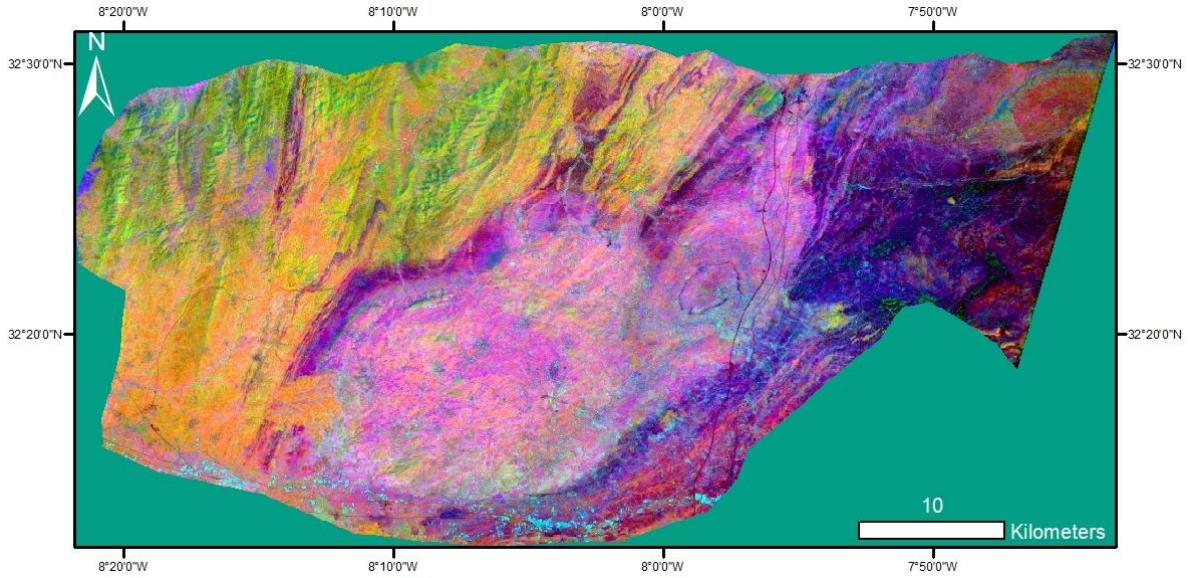

Fig.13. RGB colour combination of MNF 1-2-3 components

* elmimouni2@gmail.com

From this MNF transformation (figure 13), we notice a good discrimination of the three structural zones of the Rehamna massif and fault zones. The areas of interest appear in a blue green color (tiffany blue). Nevertheless, this method did not lead to the desired result.

Our field investigations allowed us to discover new mining occurrences at the scale of the study area (Figure 14 and Figure 15). Several indices sampled in the field are in agreement with the areas selected by image processing.

6. Field work and results

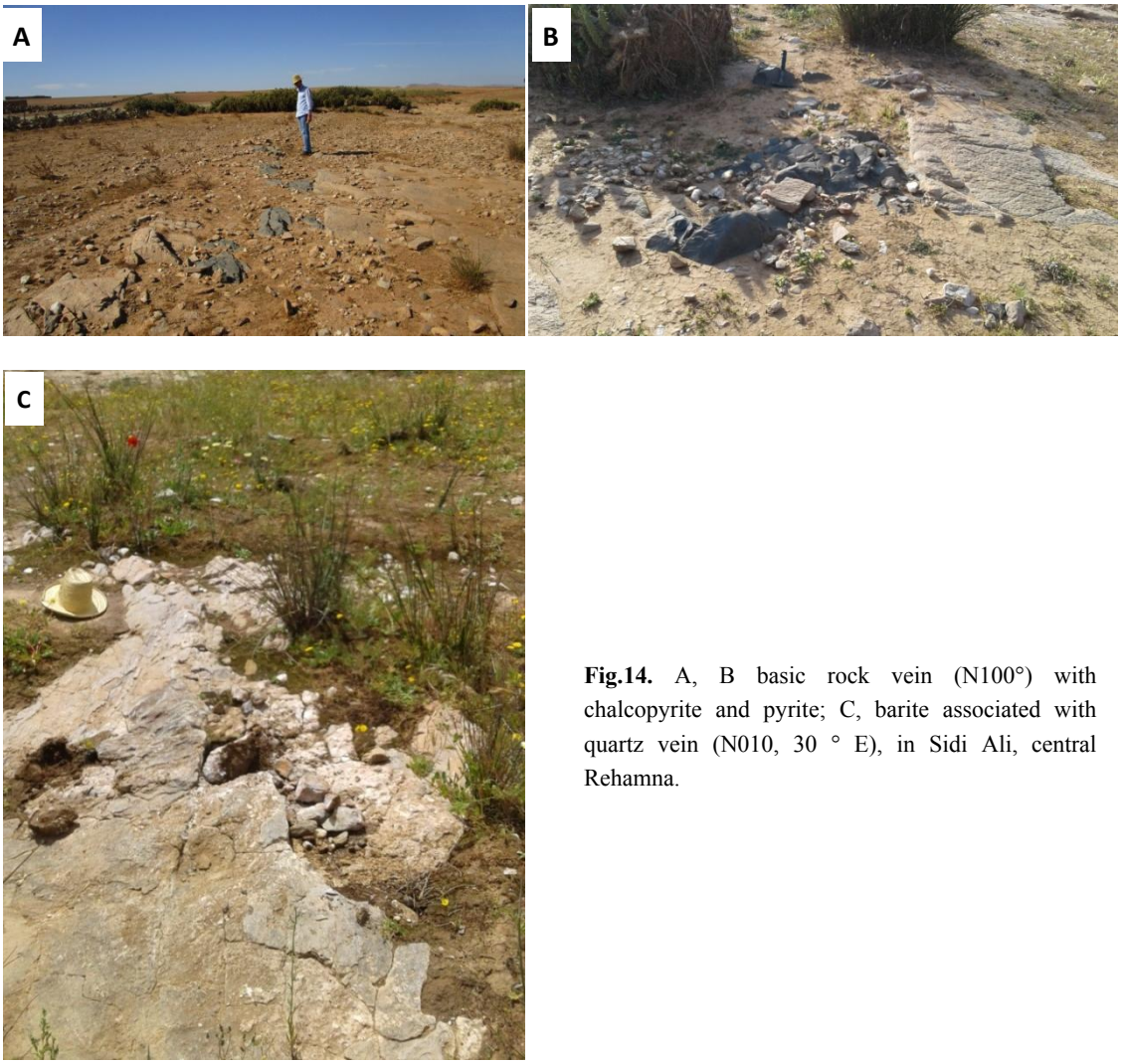

Fig.14. A, B basic rock vein (N100°) with chalcopyrite and pyrite; C, barite associated with quartz vein (N010, 30 ° E), in Sidi Ali, central Rehamna.

* elmimouni2@gmail.com

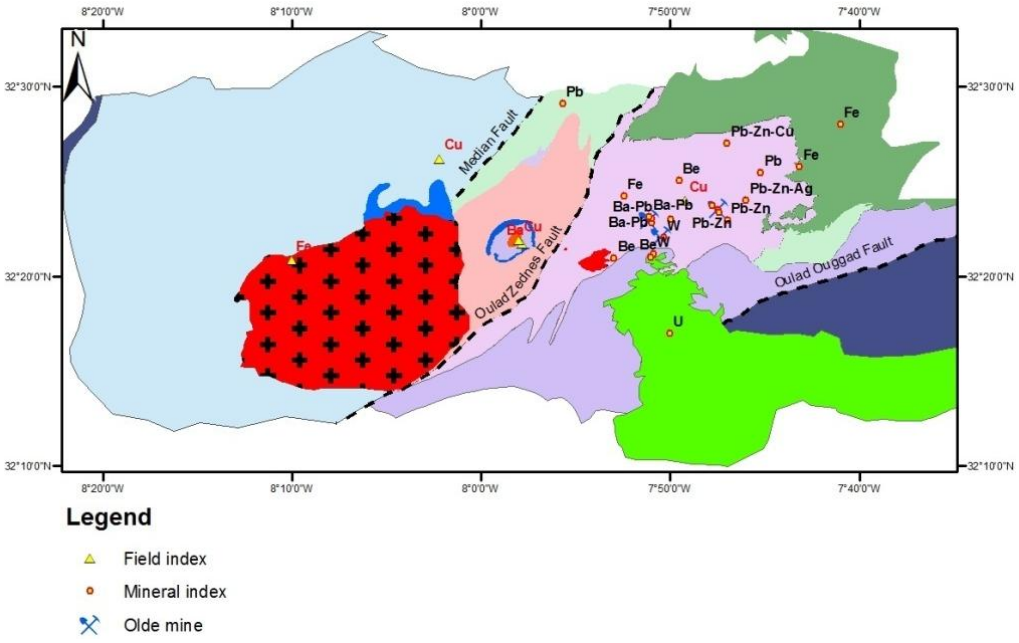

Fig. 15. Distribution of mining indices in the Rehamna Massif s.str. (Mineral index: known mineral index, Field index: new mineral index).

7. Conclusion

The synergy of both remote sensing and field data in the Rehamna Massif allowed us to draw the following conclusions.

Field investigations revealed the existence of sulphide mineralization. The minerals we were able to collect (pyrite, chalcopyrite, goethite) are related to the magmatic bodies. The position of the field indices is confirmed by the existence of the mining indices polygons obtained by image data processing. The method of processing supported by VNIR and SWIR band ratios, in the Rehamna Massif reveals a potential mining capital in relation to the indices thus demonstrated. The ACP, and MNF treatments report results converge to almost the same areas. The band ratio method is very efficiency rather than other methods uses in this study.

The localization of the zones with mining occurences shows an association with a structural component that are the faults. It also shows an association with the lithologic component mainly in granite margins and the basic vein magmatic bodies.

This study can be considered as a support and orientation for exploration and mining research in this Rehamna area. It can be fortified by other geophysical methods.

References

1. Tommaso I. Di, Rubinstein N, hydrothermal alteration mapping using ASTER data in the Infiernillo porphyry deposit, Argentina / *Ore Geology Reviews* **32** 275–290 (2007).
2. Gabr S, Ghulam A, Kusky T Detecting areas of high-potential gold mineralization using ASTER data, *Ore Geology Reviews* **38** 59–69 (2010).
3. Zhang T, Yi G, Li H, Wang Z, Tang J Li Y, Wang Q, Bie X, 2016. Integrating Data of ASTER and Landsat-8 OLI (AO) for Hydrothermal Alteration Mineral Mapping in Duolong Porphyry Cu-Au Deposit, Tibetan Plateau, China. *Remote Sens*. (2016).
4. Ramadan, T.M., Abdelsalam, M.G., Stern, R.J.,. Mapping gold-bearing massive sulfide deposits in the Neoproterozoic Allaqi suture, SE Egypt with Landsat TM and SIR-C/X-SAR images. *Photogrammetric Engineering and Remote Sensing* **67**, 491–497 (2001).
5. Ninomiya, Y. Lithological mapping with ASTER TIR and SWIR data. Proc. SPIE 5234, 180–190 (2004).
6. Michard, A coordinateur. Le massif paléozoïque des Rehamna (Maroc). Stratigraphie, tectonique et pétrogenèse d'un segment de la chaîne varisque. Notes Memoires Service Géologique Maroc **303**, 180p (1982).
7. El Kamel F. Géologie du paléozoïque des Rehamna nord-orientaux, Maroc. Evolution sédimentaire et structuration hercynienne d'un bassin dévono-carbonifère. Sédimentation et déformation des molasses post-orogénique. Tectonique. Thèse 311p. Université Paul Cézanne – Aix Marseille III, (1987).
8. Corsini, M.. Lithostratigraphie et tectonique des terrains paléozoïques dans les Rehamna et la

* elmimouni2@gmail.com

Méséta côtière. (Meseta marocaine hercynienne). Thèse 150p. Université AiX-Marseille (1988).
9. Aghzer, A. M.. Evolution tectonothermale du massif hercynien des Rehamna (Zone mésétienne centrale, Maroc). Thèse 358p. Université Com-plutense, Madrid (1994).
10. El Mahi, B. ; Hoepffner, Ch. ; Zahraoui, M. & Boushaba, A. L'évolution tectono-métamorphique de la zone hercynienne des Rehamna centraux (Maroc). Bull. Inst. Sci., Rabat, n°**22**, pp. 41-57 (1999-2000).
11. Gigout M. Etudes géologiques sur la méséta marocaine occidentale (arrière-pays de casablanca, Mazagan et Safi). Trav. Inst. Cherif., Rabat. 3, et Notes et Mém. Sérv. Géol. Maroc, **86**. 570p (1951).
12. Baudin T., Chévremont P., Razin P., Youbi N., Andries D., Hoepffner C., Thiéblemont D., Chihani E.M. & Tegyey M.. Carte Géologique du Maroc au 1/50 000 : Feuille de Skhour des Rehamna – Mémoire explicatif. Notes Mém. Serv. Géol. Maroc, vol. **435bis**, 114 p. (2003).
13. Cocherie A. Datations effectuées dans le cadre du projet Maroc. Compte-rendu technique BRGM, AC/81.11.01, 7 p. + annexes (2001).
14. Piqué, A. Contribution à la géologie structurale des Rehamna (Méséta marocaine méridionale). Le matériel paléozoïque et son évolution hercynienne dans l'Ouest du massif. Thèse 3ème cycle 101p. Université Louis-Pasteur, Strasbourg (1972).
15. Michard A., Soulaimani A., Hoepffner C., Ouanaimi H., Baidder L., Rjimati E.C., Saddiqi O, (2010) The South-Western Branch of the Variscan Belt: Evidence from Morocco, Tectonophysics 492 1–24 (2010).
16. Hoeppfner, C. Contribution à la géologie structurale des Rehamna (Méséta marocaine méridionale); le matériel paléozoïque et son évolution hercynienne dans l'Est du Massif. Thèse 3ème cycle 92p. Université Louis-Pasteur, Strasbourg (1974).
17. Michard A, Saddiqi O, Chalouan A, Rjimati E, Mouttaqi A (eds) Nouveaux guides géologiques et miniers du Maroc. Notes et mémoires du service géologique n° **563**, 121p (2011).
18. Lehmann W. Rapport géologique, bilan de minerais et premiers résultats concernant la technique de traitement. Gisement de wolfram (scheelite et wolframite). Sidi Bou Azzouz - Rehamna. Rapport inédit de la société Klœckner & Co., Rabat, 54 p. (1981).
19. Snœp J. – P Note sur une première connaissance des anomalies magnétiques des Rehamna et sur le microdosage pour Pb, Zn et Cu de ses indices de fer. Rapport BRPM, Rabat, 6 p. + 2 tabl. (1967).
20. Chauris L. et Huvelin P. Présence de béryl dans les Rehamna (Maroc). C.R. Somm. *Soc. Géol. Fr*., **8**, pp. 325326 (1964).
21. Jenny P. Contribution à la géologie structurale des Rehamna (Meseta marocaine méridionale). Le matériel paléozoïque et son évolution hercynienne dans le centre du massif. Thèse 3 cycle, Univ. Louis Pasteur, Strasbourg, 120 p. (1974).
22. Marconnet B., Gagny. C, Boushaba A. Bouybaouene M. Prospection d'apex leucogranitiques minéralisés en tungstène télédétection spatiale. Utilisation d'un phénomène de «transparence » d'une couverture métamorphique dans le massif des Rehamna (Maroc). *Chrun. rech- min*., n° **486** , pp. 63-71 (1987).
23. Rajendran S., Nasir S. Characterization of STER spectral bands for mapping of alteration zones of volcanogenic massive sulphide deposits / *Ore Geology Reviews* **88**, 317–335 (2017).
24. Rowan, L.C., Mars, J.C., Lithologic mapping in the Mountain Pass Area, California using advanced space borne thermal emission and reflection radiometer (ASTER) data. *Remote Sens. Environ*. **84**, 350–366 (2003).
25. Hewson, R.D., Cudahy, T.J., Mizuhiko, S., Ueda, K., Mauger, A.J., Seamless geological map generation using ASTER in the Broken Hill-Curnamona province of Australia. *Remote Sens. Environ*. **99**, 159–172 (2005).
26. Ninomiya, Y., A stabilized vegetation index and several mineralogic indices defined for ASTER VNIR and SWIR data. Proceedings of IEEE International Geoscience and Remote Sensing Symposium: *IGARSS'03*, **3**, pp. 1552–1554. (2003).
27. Beiranvnd Pour A., And Hashim. M. Spectral transformation of ASTER data and the discrimination of hydrothermal alteration minerals in a semi-arid region, SE Iran. *International Journal of the Physical Sciences* Vol. **6**(**8**), pp. 2037-2059 (2011).
28. Loughlin WP Principal component analysis for alteration mapping, *Journal Photogrammetric Engineering and Remote Sensing* **57**, 1163–1169. (1991).
29. Abrams MJ, Ashley RP, Brown LC, Goetz AFH, Kahle AB, Mapping of hydrothermal alteration in the Cuprite mining district, Nevada, using aircraft scanning images for the spectral region 0.46 to 2.36 mm. *Geology* **5**, 713–718 (1997).
30. Tangestani MH, Moore F. Comparison of three principal component analysis techniques to porphyry copper alteration mapping: a case study, Meiduk area, Kerman, Iran. *Canadian Journal of remote Sensing* **27**, 176–181 (2001).

* elmimouni2@gmail.com

31. Boardman, J.W. and Kruse. F.A. Automated spectral analysis: A geological example using AVIRIS data, Northern Grapevine Mountains, Nevada: In Proceeding Tenth Thematic Conference. *Geological Remote Sensing*, 9-12 May, San Antonio, Texas, 407-418 (1994).
32. Altinbas U, Kuruc U Y, Bolca M, El-nahry A. H Using Advanced Spectral Analyses Techniques as Possible Means of Identifying Clay Minerals Turk J Agric For 29, 19-28. (2005).

* elmimouni2@gmail.com